Received: 5 April 2025 | Revised: 9 June 2025 | Accepted: 12 June 2025 | Published online: 3 July 2025

RESEARCH ARTICLE

Smart Wearable Technology
2025, Vol. 00(00) 1–7
DOI: 10.47852/bonviewSWT52025851

BON VIEW PUBLISHING

Tunable Graphene-Based Wave Absorber: Combined Electrical and Mechanical Tuning

Amir Ali Mohammad Khani[1], Alireza Barati Haghverdi[2], Ilghar Rezaei[3], Seyed Javad Hosseini Zoljalali[4] and Toktam Aghaee[5,*]

[1]*Department of Electrical and Electronic Engineering, Islamic Azad University, Saveh Branch, Iran*

[2]*Department of Civil Engineering, Asrar Institute of Higher Education of Mashhad, Iran*

[3]*Department of Electrical and Electronic Engineering, Islamic Azad University, Central Tehran Branch, Iran*

[4]*Department of Physics, Ferdowsi Univesity of Mashhad, Iran*

[5]*Department of Electrical and Electronics Engineering, Semnan University, Iran*

Abstract: Here in this work, a graphene-based absorber in THz waves is introduced. The structure exploits the mechanical adjusting setup using a Micro-Electro-Mechanical Systems comb driver. In addition, the periodic graphene rings and disks are used on top of the TOPAS (cyclic olefin copolymer) spacer. The middle layer spacer is considered as an air gap that can be filled by any target samples. The mechanical tuning besides the influence of the chemical potential makes the proposed structure most tunable with more than five absorption peaks in the THz gap. Two parallel simulation paths are followed in this work. First, an equivalent circuit model representation is developed, and the absorption response is obtained by leveraging the impedance matching theorem. Then the full-wave numerical modeling via the finite element method is performed to investigate the first approach's validity and accuracy. It is shown that combining electrical and mechanical stimulations can change the number of absorption peaks and also their frequencies. According to the simulation results, the proposed absorber is highly reliable and robust against probable geometrical mismatches, while almost all of the THz spectrum is covered by the proposed structure.

Keywords: graphene, graphene-based terahertz, absorber, circuit model, sensor

1. Introduction

Graphene is a single-atom-thick layer of carbon atoms arranged in a two-dimensional honeycomb lattice, known for its extraordinary properties. It is about 200 times stronger than steel while being extremely lightweight and flexible. Graphene exhibits exceptional electrical and thermal conductivity, with electrons moving at near-light speeds on its surface. Despite its thinness, it is nearly transparent and chemically stable. First isolated in 2004 by Andre Geim and Konstantin Novoselov, who later won the Nobel Prize, graphene's unique structure makes it ideal for applications in electronics, energy storage, biomedicine, and advanced composites. Its scalable production methods are advancing, promising widespread industrial use in the near future [1].

Graphene-based terahertz (THz) absorbers have emerged as highly promising devices due to graphene's unique electronic and optical properties, such as tunable surface conductivity and strong plasmonic resonances in the THz frequency range. These absorbers typically consist of patterned graphene layers combined with dielectric spacers and metallic back reflectors, forming metasurface or metamaterial structures that achieve near-perfect absorption at designed frequencies. By adjusting parameters like graphene's chemical potential, layer geometry, and dielectric properties, these absorbers can exhibit multi-band, broadband, and polarization-insensitive absorption with efficiencies often exceeding 90–99% across wide THz bandwidths. Such features make graphene-based THz absorbers attractive for applications in sensing, imaging, communication, and security screening [2].

The physical mechanism underlying absorption in these devices relies on the excitation of graphene surface plasmons, which are highly confined electromagnetic modes tunable via electrostatic gating or chemical doping. This tunability allows dynamic control over resonance frequencies and absorption intensities, enabling adjustable bandwidths and multi-band operation. Recent designs incorporate multilayer graphene metasurfaces, hybrid materials, and novel patterns (e.g., oval-shaped or nested nanostructures) to enhance absorption bandwidth and angular stability. Moreover, graphene absorbers demonstrate robustness against polarization and incident angle variations, making them versatile for practical THz systems. Advances in integrating graphene with Micro-Electro-Mechanical Systems (MEMS) actuators and novel dielectrics further expand their functional tunability and adaptability for next-generation THz technologies [3].

Mechanical tuning for graphene-based absorbers has been extensively explored in recent research. Various studies have proposed innovative approaches to achieve mechanical and

*Corresponding author: Toktam Aghaee, Department of Electrical and Electronics Engineering, Semnan University, Iran. Email: Toktam.Aghaee@semnan.ac.ir

electrically tunable infrared absorbers using graphene structures [4]. Additionally, the concept of reconfigurable metasurfaces for optical absorption modulation has been introduced, highlighting the critical coupling of resonance modes and plasma dispersion effects in semiconductors for fast tunability [5]. Furthermore, a basic tunable absorber based on graphene with a tunable Fermi level has been designed to address the limitations of conventional noble metal absorbers, displaying the capacity to alter absorption frequency by controlling relaxation time, Fermi level, or refractive index of the medium [6]. In addition, a graphene-based absorber in a microwave with an electrically tunable absorption frequency has been proposed, demonstrating a wide tunable range and high absorption rates, suitable for applications in electromagnetic protection and stealth [7].

Tunability remains a cornerstone of graphene-based absorber design, with impedance matching adjusted via electrical, thermal, or chemical means. For instance, dual-tunable absorbers combining graphene and Dirac semimetals achieve 90% absorption from 4.06 to 10.7 THz by independently modulating Fermi energy and permittivity. Patterned graphene structures also allow frequency-selective absorption, with absorption rates adjustable from >97% reflection to 86.7% absorption by varying graphene's chemical potential. These innovations underscore graphene's versatility in THz applications, from electromagnetic shielding to imaging, where adaptive impedance matching ensures optimal performance across diverse operational requirements [8].

Wearable sensors leveraging graphene and flexible dielectrics combine advanced material properties for next-generation health monitoring. Graphene's exceptional electrical conductivity, mechanical flexibility, and biocompatibility enable seamless integration with human skin, improving signal quality for physiological tracking. Flexible dielectric materials like thermoplastic polyurethane or polydimethylsiloxane enhance sensor sensitivity by optimizing capacitance changes under mechanical stress. These composites often feature microstructured surfaces or porous architectures, such as 3D graphene foams, which amplify responsiveness to pressure, strain, or temperature variations while maintaining durability during repeated deformations [9].

In health applications, graphene-based sensors detect vital signs like pulse, respiration, and muscle activity through electrophysiological or mechanical sensing. For example, capacitive pressure sensors with graphene-enhanced dielectric layers achieve high sensitivity (0.28 kPa^{-1}) and fast response times (~65 ms), enabling precise monitoring of limb movements or object grasping forces4. Hybrid systems integrating graphene with carbon nanotubes or nanocellulose further improve stretchability (up to 150% strain) and thermal stability, allowing real-time tracking during daily activities without motion artifacts. Such devices are increasingly used in wearable patches, smart textiles, and implantable systems for chronic disease management [10].

Scalable manufacturing and sustainability remain key challenges. Recent advances employ cost-effective methods like electrospinning stainless steel templates or recycled materials (e.g., alum sludge) to produce flexible dielectrics. Innovations in microwave reflectometry enable rapid characterization of ultra-thin biopolymer films, ensuring consistent dielectric properties for mass production. While graphene composites like PAN/GO nanofibers demonstrate high permittivity ($\varepsilon_r = 86.4$) and mechanical strength, ongoing research focuses on reducing hysteresis and enhancing environmental resilience for long-term wearability. These developments position graphene-dielectric sensors as critical tools for personalized healthcare and human–machine interfaces [11, 12].

Here in this work, a multilayers graphene-based THz absorber is investigated. The proposed structure is discussed in the next section with details of circuit modeling and impedance matching. Then Section 3 reports simulation results from circuit modeling and numerical full-wave approach. Both stimulations in this work are external factors including electrical gate biasing and mechanical tuning. So absorption curves under different stimulations are reported in this section. Finally, the work is concluded in Section 4.

2. Proposed Structure

Three types of materials including gold, TOPAS (cyclic olefin copolymer), and graphene form the proposed absorber. The top and perspective views of the presented absorber are demonstrated in Figure 1. The top layer is equipped with a movable frame, while the frame can move horizontally by a MEMS comb driver. Additionally, the second spacer layer is considered an air gap.

The TOPAS spacer layer plays a critical role in optimizing impedance matching and broadband absorption performance in graphene-based THz absorbers. As a low-loss dielectric with a refractive index of 1.53 and dielectric constant of 2.35 in the THz range, TOPAS enables precise control over electromagnetic wave interference patterns. In the demonstrated absorber design, a 16 μm TOPAS layer between two patterned graphene sheets creates destructive interference conditions that suppress reflection while enhancing absorption bandwidth. This thickness aligns with interference cancellation theory requirements, where $d \sim \lambda/(4\sqrt{\varepsilon})$ matches the 94.3 μm wavelength at 3.18 THz. The spacer's optimized dimensions allow simultaneous excitation of localized surface plasmons and propagating surface plasmons, achieving >90% absorption across 1.91–4.45 THz through hybrid resonance effects [13, 14].

TOPAS provides a good balance of low loss and processability; however, alternative dielectrics like GaAs and SiO_2 could offer improved impedance matching, tunability, and bandwidth in graphene-based THz absorbers. The choice of spacer material directly affects absorption efficiency, bandwidth, and tunability, and exploring these alternatives could yield absorbers with enhanced or more application-specific performance characteristics [15, 16]. In addition, Table 1 shows the geometric dimensions of the proposed graphene-based sensor.

To model graphene patterns into circuit elements according to the equivalent circuit model (ECM) view, every layer of the graphene pattern is treated as an endless series of R-L-C branches. Consequently, the layers composed of graphene disks and graphene rings incorporate R-L-C branches as represented in Equations (1) and (2), respectively. In addition, graphene surface conductivity is expressed by Equation (3) [17].

$$R_n = \frac{L^2 K_n}{\pi S_n^2}\frac{\hbar^2}{e^2 E_F \tau}, L_n = R_n \tau, C_n = \frac{\pi^2 S_n^2}{L^2 K_n}\frac{\varepsilon_{eff}}{q_{1n}} \tag{1}$$

$$R_n = \frac{S_{cell} P_n}{\pi^2}\mathrm{Re}[\sigma_s{}^{-1}], L_n = \frac{S_{cell} P_n}{\pi^2}\frac{\mathrm{Im}[\sigma_s{}^{-1}]}{\omega}, C_n = \frac{\pi^2}{S_{cell} P_n}\frac{\varepsilon_{eff}}{q_{1n}} \tag{2}$$

$$\sigma_s = -\frac{je^2 K_B T \tau}{\pi\hbar^2(\omega - 2j)}\left(\frac{\mu_c}{K_B T} + 2\ln\left(\frac{1}{e^{\frac{\mu_c}{K_B T}}} + 1\right)\right) \tag{3}$$

where *Rn*, *Cn*, and *Ln* are equivalent resistance, inductor, and capacitor, respectively. Additionally, εeff is the effective permittivity and is indicated as $(\varepsilon 1 + \varepsilon 2)/2$, where $\varepsilon 1$ and $\varepsilon 2$ are the upper and lower material permittivity, respectively. τ is electron relaxation. μc is chemical potentials. Also, *EF* is Fermi's energy level. ħ is the reduced Plank constant. In addition, *Scell* is the area

Figure 1
Proposed wave absorber from top view (mechanical tuning) and perspective view (unit cell)

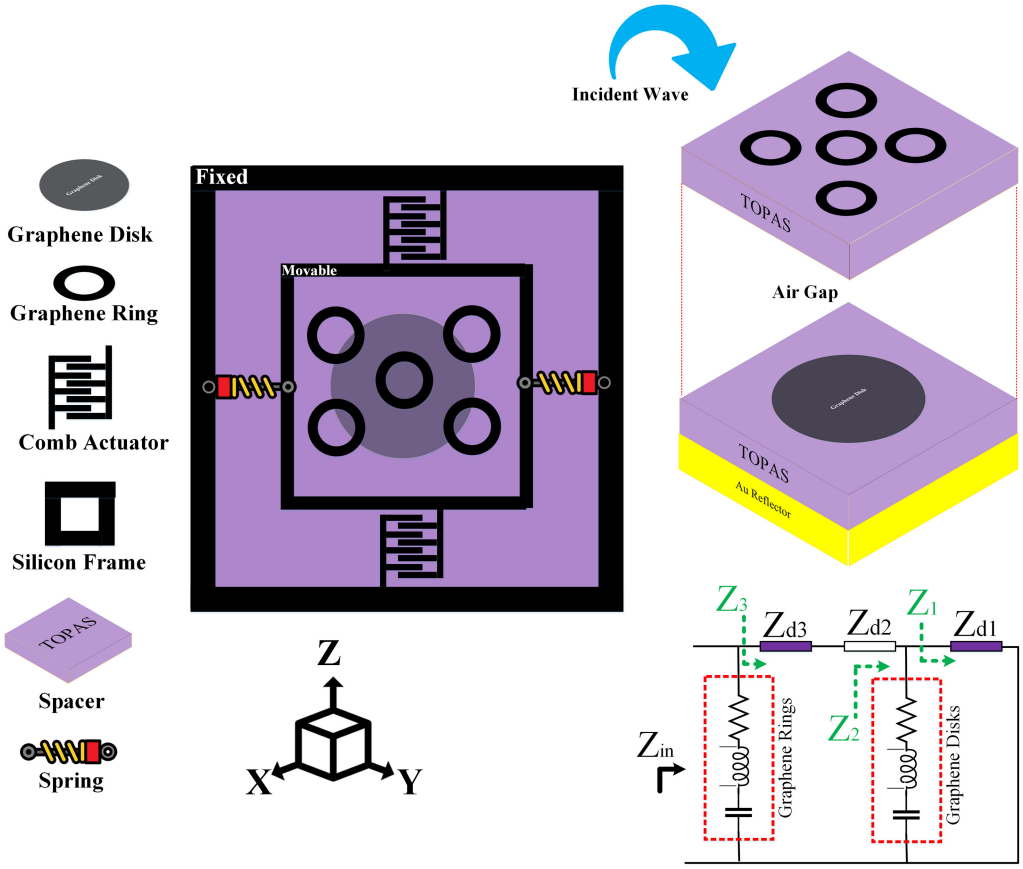

Table 1
The geometric dimensions of the proposed graphene-based sensor

Parameter	Value (μm)	Definition
a	6	The radius of the graphene disks
L	18	The period of graphene disks
rin	8	The inner radius of graphene rings
rout	12	The outer radius of graphene rings
d1	14	The thicknesses of the first dielectric layer (TOPAS)
d2	22	The thicknesses of the second dielectric layer
d3	12	The thicknesses of the third dielectric layer (TOPAS)
tAu	1 μm	The thickness of the gold layer
tg	1 nm (3 × 0.32 nm)	The thickness of the graphene layer (three carbon atoms)

of one cell of the periodic structure. So, *Pn*, *Kn*, and *Sn* are eigenfunctions. Additionally, $q1n$ is the eigenvalue. Furthermore, KB is Boltzmann's constant, and e is the charge of an electron. Finally, T is temperature.

To place each circuit element in the ECM of the proposed structure, the gold layer is viewed as a short circuit because of its reflective characteristics. Moreover, the dielectric layer is treated as a series component because of its thickness. Consequently, the graphene patterns are regarded as parallel components in ECM due to their extremely thin thickness. Consequently, the input impedance (Zin) of the proposed absorber is articulated by Equation (4)–(7) [17].

$$Z_1 = jZ_{d1}\tan(bd_1) \tag{4}$$

$$Z_2 = Z_{G-Disks} \| Z_1 \tag{5}$$

$$Z_3 = (Z_{d2} + Z_{d3})\frac{Z_2 + j(Z_{d2} + Z_{d3})\tan(b(d_2 + d_3))}{(Z_{d2} + Z_{d3}) + jZ_2.\tan(b(d_2 + d_3))} \tag{6}$$

$$Z_{in} = Z_{G-Rings} \| Z_3 \tag{7}$$

where β is the propagation constant in the dielectric. ZG-Disks and ZG-Dings are the equivalent impedance of graphene patterns and are also calculated as $ZG = 1/\sigma G$. In addition, Zd is the equivalent impedance of the dielectric and is expressed by $Zd = Z0/n$. Since $d1$ and $d3$ are filled with TOPAS, so $n1, 3 = 1.61$. Also, $d2$ is filled with air, so $n2 = 1$.

The absorption is expressed as Equation (8), which, if the real part (Zin)~$Z0 = 120\pi\ \Omega$ and the imaginary part (Zin)~0, then maximum absorption can be acquired [17].

$$R = \frac{(Z_{in} - Z_0)}{(Z_{in} + Z_0)} \qquad (8)$$
$$A = 1 - |R|^2$$

where R is reflection and A is absorption.

The next section reports the simulation results of the proposed sensor.

3. Simulation Results

The demonstrated unit cell in Figure 1 is simulated using CST software and the finite element method (FEM), where frequency domain solver with Floquet port boundary conditions is considered to extract the performance of the device. The Floquet port, where the unit cell is placed in the x and y directions and free space in the z-direction, is exploited exclusively with a planar periodic arrangement. In the z-axis, a perfectly matched layer is exploited to ensure zero scattering, leading to the accuracy of the results. The analysis of the infinite structure is then performed by analyzing a unit cell. Linked boundaries most often form the sidewalls of a unit cell, but in addition, a boundary condition is needed to consider the infinite space above. The Floquet port is designed for this end. Boundaries that are adjacent to a Floquet port must be linked boundaries. The tetrahedral mesh type having adaptive mesh refinement is selected, and the mesh subdivides the structure into a large number of tetrahedrons, which is required to achieve the desired simulation accuracy. To ensure zero transmission, the gold dispersive medium with a thickness larger than the penetration depth of THz is used [17].

Additionally, the calculated impedance from the ECM is investigated in Figures 2 and 3. According to the developed ECM, the equivalent impedance of the absorber is a complex value. The impedance map shown in Figure 2 obviously highlights the perfect matching point (real = 120 πΩ and imaginary = 0) by red-dots convergence. Figure 2 highlights the potential capability of the calculated impedance for maximum power transfer.

Furthermore, the impedance is also shown against the THz gap in Figure 3. Based on real and imaginary impedance curves in the figure, it is predicted that the proposed absorber will show high absorption rates at the matching points.

To investigate the validity and accuracy of the ECM, Figure 4 is reported extracted from the FEM simulation. This figure reports the absorption against the oblique incident. As predicted, the absorption peaks were placed exactly in matched points. These results verify both the ECM accuracy and also state the excellent performance of the proposed absorber dealing with oblique incidents. Furthermore, absorption against horizontal shifts from −2 μm to 2 μm is shown in Figure 5. The horizontal shifts of the upper layer can cause enhancing absorption peaks.

The absorption sensitivity of graphene-based THz absorbers tuned via MEMS-driven horizontal shifts is primarily governed by the near-field coupling between graphene meta-atoms and the underlying substrate or adjacent layers. When a MEMS actuator laterally displaces the top graphene layer relative to a fixed bottom layer, it modifies the overlap and alignment of periodic graphene patterns, which in turn alters the localized plasmonic resonances responsible for strong absorption. This mechanical tuning can induce significant shifts in the resonance frequency and changes in absorption intensity. Furthermore, the absorption response to horizontal shifts via MEMS actuation shows a nonlinear dependence on displacement due to the complex electromagnetic coupling in the metamaterial structure. As the graphene layers move out of perfect alignment, symmetry breaking excites additional plasmonic modes, broadening the absorption bandwidth and increasing modulation contrast. The tuning range and sensitivity are also influenced by the design of the graphene patterns (e.g., disks, ribbons) and the dielectric environment. MEMS-driven horizontal tuning offers fast

Figure 2
Impedance map

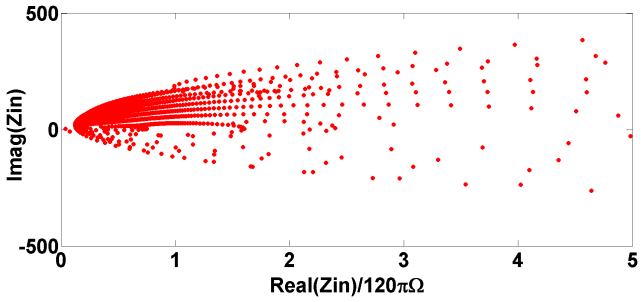

Figure 3
Impedance counterparts against frequency

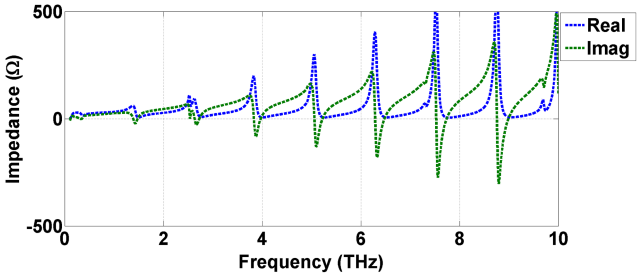

Figure 4
Absorption per oblique incident

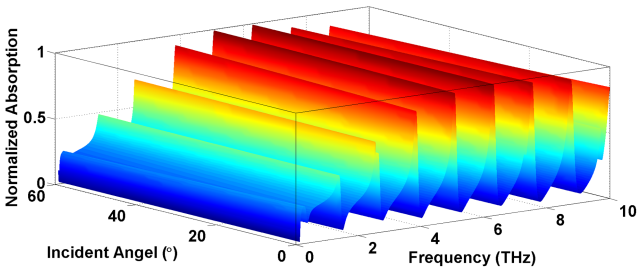

Figure 5
Absorption versus horizontal shifts in Y direction

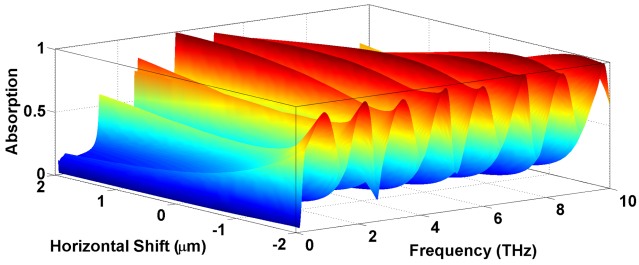

Figure 6
Absorption per different horizontal shifts and chemical potentials

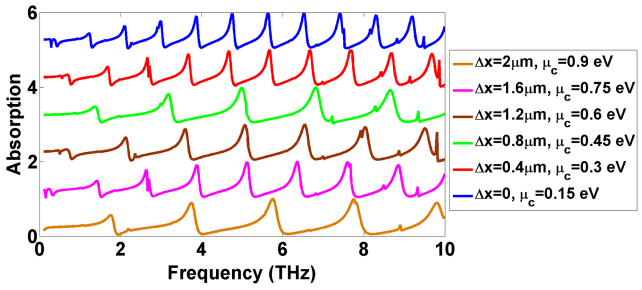

switching speeds (on the order of microseconds) and precise control, making it suitable for dynamic THz devices. However, optimizing the trade-off between maximum absorption, tuning range, and mechanical stability remains an ongoing challenge in device development [18–20].

Finally, by combining the mechanical and electrical stimulations, different shapes and peaks in the absorption response can be achieved, as shown in Figure 6. In this view, the absorption curve can be tuned to any desired frequency. This capability is in high demand for several applications, and the proposed absorber can act as the basic building block for numerous sensing systems.

Mechanical adjustments alter the geometric configuration of graphene structures, modifying plasmonic resonance conditions. Horizontal shifts change the effective conductivity by varying the overlap area between upper and lower nanoribbon arrays. This modifies surface plasmon polariton coupling, leading to absorption peak shifts. Lateral displacement of graphene disks relative to a fixed layer alters the effective periodicity, shifting resonant frequencies.

Further to investigate the geometrical variations and their effects on absorption response, Figures 7–9 are reported. These figures are shown to highlight the robustness and reliability of the proposed absorber against geometrical mismatches and possible fabrication errors. In this regard, Figure 6 considers changeable graphene disks with different radiuses and periods. Additionally, the graphene ring is investigated, while the layers' thickness effects on absorption are demonstrated in Figure 9. According to these figures, while the proposed absorber is highly adjustable via external stimulation, it is completely reliable against possible mismatches by keeping the same response shapes with negligible errors.

Finally, the work is compared with other existing absorbers to highlight its performance in Table 2.

Figure 7
Absorption deviation versus graphene disk geometry

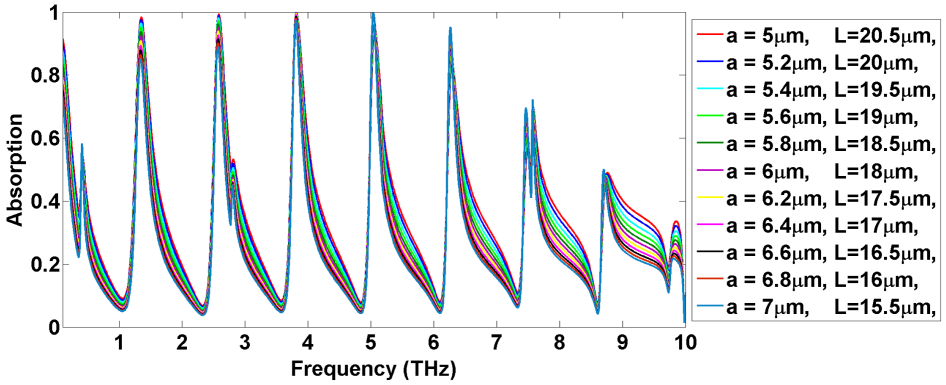

Figure 8
Absorption deviation versus the graphene ring geometry

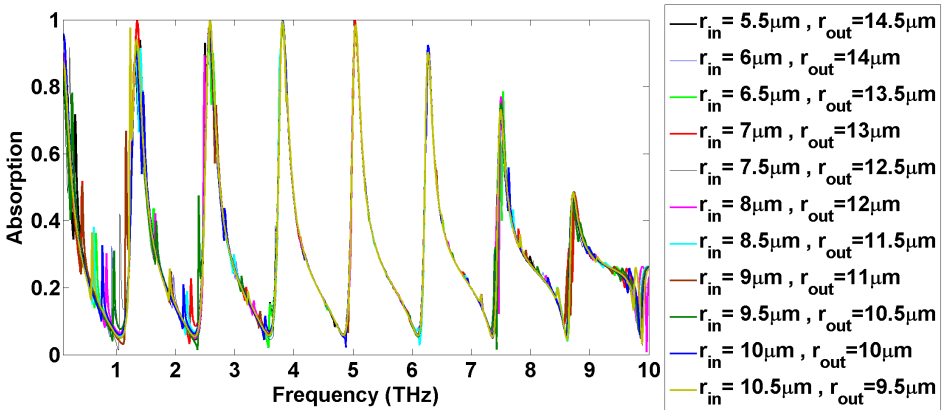

Figure 9
Absorption deviation versus layers thicknesses

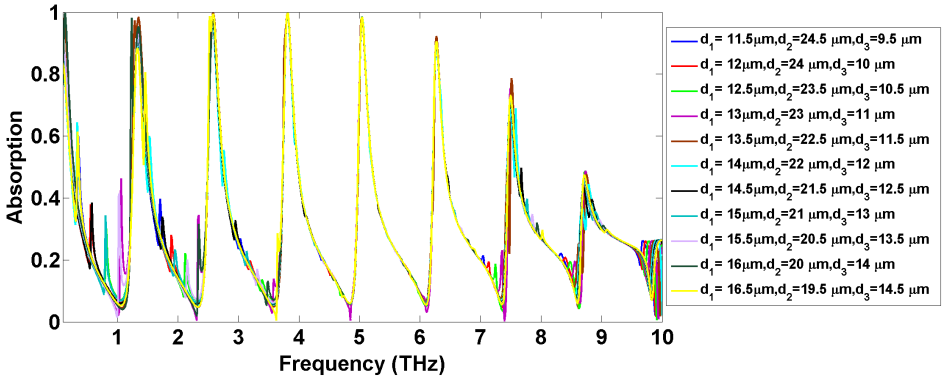

Table 2
Absorption deviation versus layers thicknesses

	Reconfigurable	Adjusting method	Device height	Tuning range
[1]	Yes	Electrical	39 μm	0.2 THz
[2]	No	Electrical	70 μm	2 THz
[3]	No	Electrical	125 μm	5 GHz
[4]	No	Electrical	34 μm	2 THz
This work	Yes	Combined Electrical and mechanical	49 μm	2–9 THz full covering with over 90% Absorption

4. Conclusion

A mechanical adjusting method is applied to a THz wave absorber with a combination of electrical gate biasing. The absorber itself exploits three stacked layers, while the middle layer is an air gap. The whole structure is represented by a developed ECM, while the unit cell of the device is simulated via the numerical FEM. Excellence convergence between the ECM and the FEM verifies the superior performance of the equivalent circuit modeling. Additionally, the proposed absorber includes overall of the THz gap. In addition, detailed sensitivity investigations demonstrate the dependability and strength of the suggested absorber. While the proposed absorber expresses acceptable and reliable behavior against geometrical parameters, the absorption response is highly sensitive to external stimulations with both peak numbers and their frequencies. Such capability in being tuned is in great demand to form larger optical systems including biomedical sensors and industrial detectors.

Ethical Statement

This study does not contain any studies with human or animal subjects performed by any of the authors.

Conflicts of Interest

The authors declare that they have no conflicts of interest to this work.

Data Availability Statement

Data available on request from the corresponding author upon reasonable request.

Author Contribution Statement

Amir Ali Mohammad Khani: Software, Resources. **Alireza Barati Haghverdi:** Methodology, Formal analysis. **Ilghar Rezaei:** Validation, Investigation. **Seyed Javad Hosseini Zoljalali:** Conceptualization, Data curation, Visualization. **Toktam Aghaee:** Writing – original draft, Writing – review & editing, Supervision, Project administration.

References

[1] Liao, S., Sui, J., & Zhang, H. (2022). Switchable ultra-broadband absorption and polarization conversion metastructure controlled by light. *Optics Express*, *30*(19), 34172–34187. https://doi.org/10.1364/OE.472336

[2] Barati Haghverdi, A., Rezaei, I., Mohammad Khani, A. A., & Aghaee, T. (2025). Methane detection approach based on THz wave absorber. *Sensing and Bio-Sensing Research*, *47*, 100758. https://doi.org/10.1016/j.sbsr.2025.100758

[3] Rezaei, I., Haghverdi, A. B., Soldoozy, A., Aghaee, T., & Biabanifard, S. (2024). Wearable Kapton graphene biosensor for detection of toxic gases. *Journal of Hazardous Materials Advances*, *15*, 100452. https://doi.org/10.1016/j.hazadv.2024.100452

[4] Rezapour Gatabi, M., Amiri, S. S. G., Yousefi, R., Dehbovid, H., & Afzalian, A. (2024). CO_2 sensing via periodic array of graphene disks. *Sensing and Bio-Sensing Research*, *46*, 100696. https://doi.org/10.1016/j.sbsr.2024.100696

[5] Zamzam, P., Rezaei, P., Abdulkarim, Y. I., & Mohsen Daraei, O. (2023). Graphene-based polarization-insensitive metamaterials with perfect absorption for terahertz biosensing applications: Analytical approach. *Optics & Laser Technology*, *163*, 109444. https://doi.org/10.1016/j.optlastec.2023.109444

[6] Ding, Z., Su, W., Ye, L., Wu, H., & Yao, H. (2023). An electrical/thermal dual-controlled quad-functional terahertz metasurface absorber. *Physical Chemistry Chemical Physics*, *25*(24), 16331–16339. https://doi.org/10.1039/D3CP01275A

[7] Samy, O., Belmoubarik, M., Otsuji, T., & El Moutaouakil, A. (2023). A voltage-tuned terahertz absorber based on MoS_2/graphene nanoribbon structure. *Nanomaterials*, *13*(11), 1716. https://doi.org/10.3390/nano13111716

[8] Sagadevan, K., Elizabeth Caroline, B., Lavanya, B., Lavanya, S., & Mohamed Nizar, S. (2023). Adaptable terahertz absorber using circular shaped graphene metamaterial for LO technology. In *2023 IEEE Devices for Integrated Circuit*, 302–306. https://doi.org/10.1109/DevIC57758.2023.10134847

[9] Khani, A. A. M., Haghverdi, A. B., Rezaei, I., Soldoozy, A., & Aghaee, T. (2025). Hydrogel-based THz wave absorber. *Results in Optics*, *19*, 100810. https://doi.org/10.1016/j.rio.2025.100810

[10] Rashidi, B., Rezaei, I., Soldoozy, A., Salmanpour, A., & Aghaee, T. (2024). Metasurface absorber for blood hemoglobin concentration. *ACS Applied Bio Materials*, *7*(9), 5948–5955. https://doi.org/10.1021/acsabm.4c00512

[11] Kaidarova, A., Khan, M. A., Marengo, M., Swanepoel, L., Przybysz, A., Muller, C., . . . , & Kosel, J. (2019). Wearable multifunctional printed graphene sensors. *NPJ Flexible Electronics*, *3*(1), 15. https://doi.org/10.1038/s41528-019-0061-5

[12] Xie, T., Zhang, L., Wang, Y., Wang, Y., & Wang, X. (2019). Graphene-based supercapacitors as flexible wearable sensor for monitoring pulse-beat. *Ceramics International*, *45*(2), 2516–2520. https://doi.org/10.1016/j.ceramint.2018.10.181

[13] Huang, H., Su, S., Wu, N., Wan, H., Wan, S., Bi, H., & Sun, L. (2019). Graphene-based sensors for human health monitoring. *Frontiers in Chemistry*, *7*, 399. https://doi.org/10.3389/fchem.2019.00399

[14] Qiao, Y., Li, X., Hirtz, T., Deng, G., Wei, Y., Li, M., . . . , & Ren, T. L. (2019). Graphene-based wearable sensors. *Nanoscale*, *11*(41), 18923–18945. https://doi.org/10.1039/C9NR05532K

[15] Li, R., Hu, J., Li, Y., Huang, Y., Wang, L., Huang, M., . . . , & Chen, L. (2025). Graphene-based, flexible, wearable piezoresistive sensors with high sensitivity for tiny pressure detection. *Sensors*, *25*(2), 423. https://doi.org/10.3390/s25020423

[16] Xie, B., Guo, Y., Chen, Y., Zhang, H., Xiao, J., Hou, M., . . . , & Wong, C. (2025). Advances in graphene-based electrode for triboelectric nanogenerator. *Nano-Micro Letters*, *17*(1), 17. https://doi.org/10.1007/s40820-024-01530-1

[17] Rezaei, I., Salmanpour, A., Zanjani, M. S., Biabanifard, S., & Aghaee, T. (2023). Multi-functional graphene periodic patterns. *Diamond and Related Materials*, *136*, 110003. https://doi.org/10.1016/j.diamond.2023.110003

[18] Ye, Z., Wu, P., Wang, H., Jiang, S., Huang, M., Lei, D., & Wu, F. (2023). Multimode tunable terahertz absorber based on a quarter graphene disk structure. *Results in Physics*, *48*, 106420. https://doi.org/10.1016/j.rinp.2023.106420

[19] Wang, P., Tao, H., & Wang, Q. (2022). Large range frequency-tunable transparent absorber based on patterned graphene. In *Cross Strait Radio Science & Wireless Technology Conference*, 1–3. https://doi.org/10.1109/CSRSWTC56224.2022.10098333

[20] Wu, J., Sun, Y., Wu, F., Wu, B., & Wu, X. (2022). Tunable high-quality-factor absorption in a graphene monolayer based on quasi-bound states in the continuum. *Beilstein Journal of Nanotechnology*, *13*, 675–681. https://doi.org/10.3762/bjnano.13.59

How to Cite: Khani, A. A. M., Haghverdi, A. B., Rezaei, I., Zoljalali, S. J. H., & Aghaee, T. (2025). Tunable Graphene-Based Wave Absorber: Combined Electrical and Mechanical Tuning. *Smart Wearable Technology*. https://doi.org/10.47852/bonviewSWT52025851